

# Summary of the PhD Thesis

## Contributions to LTE Implementation

Author: Jamal MOUNTASSIR

### 1. Introduction

The evolution of wireless networks process is an ongoing phenomenon. There is always a need for high data rates, reduced packet latency or delay, high spectral efficiency and lower cost. The third Generation Partnership Project Long Term Evolution (3GPP LTE) is one of the choices for next generation wireless networks. In order to achieve its target, LTE specified a new radio interface based on Orthogonal Frequency Division Multiple Access (OFDMA) in Downlink and Single Carrier Frequency Division Multiple Access (SC-FDMA) in Uplink, which is based on OFDMA implemented by Discrete Fourier Transform (DFT) precoding, along with Multiple Input Multiple Output (MIMO) antenna processing and all services are supported on IP based architectures. This new OFDMA based air interface is utilized under Evolved UMTS terrestrial Radio Access Network (E-UTRAN) and supported with a new flatter- IP core termed as Evolved Packet Core (EPC).

The principal advantage of SC-FDMA is its low Peak-to-Average Power Ratio (PAPR) of the transmitted signal. The PAPR value should be low because any power amplifier of a transmitter is nonlinear and saturates if the entry signal exceeds a certain threshold (corresponding to the big peak power value). After saturation of the power amplifier, the signal waveform is distorted resulting an Inter-symbol Interference (ISI) and the subcarriers separation becomes very difficult at the receiver.

### 2. LTE architecture

LTE introduces important changes in comparison with its precursor communication technologies, in three major areas: Air interface, Radio network Architecture, and Core Network. The LTE architecture is presented in Figure 1.

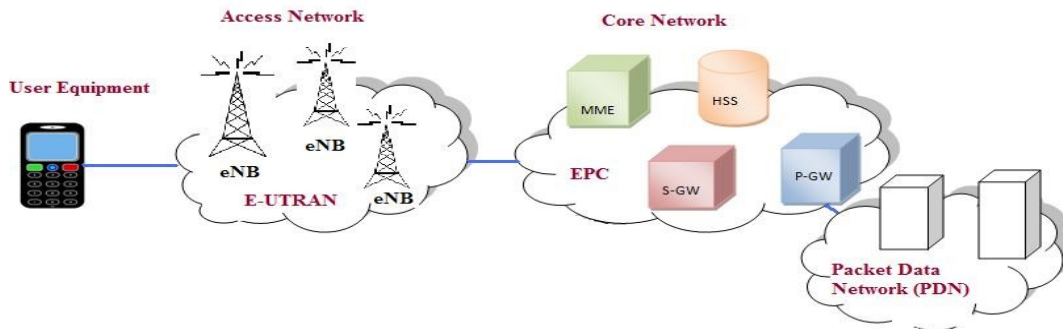


Figure 1: LTE architecture.

The Evolved UMTS Terrestrial Radio Access Network (E-UTRAN) is the radio access network of LTE. It consists only of cell sites, or evolved NodeBs (eNBs), which are the base stations of LTE and responsible to provide the E-UTRAN user plane and control plane protocol terminations towards the User Equipment (UE). The LTE architecture has only one core network defined as EPC, which is dedicated to packet data. Voice services are established like other IP packet data services as voice over IP (VoIP), typically using IMS services environment beyond the EPC. This greatly simplifies the architecture since voice is no longer handled as an exception case. The migration also enables improved internetworking with other fixed and wireless communication networks.

The EPC consists of several network elements that provide functions like the management of mobiles within its domain, authentication of subscribers and establishment of the bearer path to transport traffic between the UE and the Packet Data Network (PDN). The functions are supported in the EPC by entities like the MME, the S-GW, the PDN Gateway (P-GW), the Home subscriber Server (HSS) and the PCR (Policy and Charging Rules) function.

### 3. Multiple Access Schemes in LTE

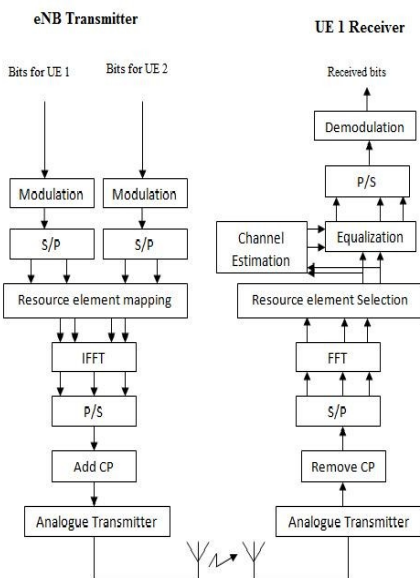


Figure 3.4: OFDMA system.

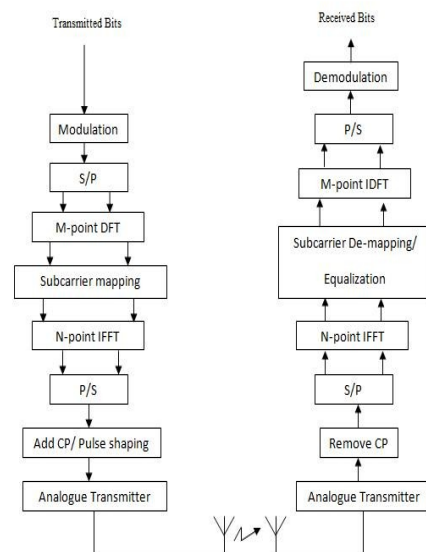


Figure 3.8: SC-FDMA system.

OFDMA allows the base station to communicate with several mobile stations at the same time. According to, OFDMA is the access multiplexing scheme for OFDM. The OFDMA inherits all the properties of the OFDM and exhibits some new features. Multiplexing provides a package of many user packets into one frame. As a result, multiplexing becomes very efficient in the sense that overheads caused by inter frame spacing is minimized. In Figure 2 is presented an OFDMA system.

Single carrier Frequency Division Multiple Access (SC-FDMA) systems utilize single carrier modulation and frequency domain equalization. SC-FDMA is a multiple access technique used in LTE Uplink. SC-FDMA is an extension of Single Carrier modulation with Frequency domain Equalization

(SC-FDE) to accommodate multiple-users access. The Peak-to-Average-Power Ratio (PAPR) in SC-FDMA, which is a typical problem in multiple access techniques, is lower than in OFDMA. In Figure 3 is presented an SC-FDMA transceiver.

### 3.4. Simulation of OFDMA and SC-FDMA in Matlab

The following results were obtained after simulation of OFDMA and SC-FDMA by considering a simple Rayleigh flat fading channel with the standard deviation equal to  $1/\sqrt{2}$  and an Additive White Gaussian Noise (AWGN) channel. We simulate the OFDMA and SC-FDMA baseband system by considering SISO system, 512 subcarriers and a CP length equal to 20.

In Figure 4 is shown the SER performance of SC-FDMA for two different subcarrier mapping schemes, IFDMA and LFDMA, in flat fading Rayleigh channel. We can observe the similarity between their SER performances.

To compare the PAPR of OFDMA and SC-FDMA, a MATLAB simulation was done with the same input parameters for both multiple access techniques. The SC-FDMA signal is passed through a raised-cosine pulse shaping filter and rectangular pulse shaping filter respectively. The OFDMA signal is not pulse shaped. We computed the Complementary Cumulative Distribution Function (CCDF) of PAPR, which is the probability that PAPR is higher than a certain PAPR value  $PAPR_0$ , ( $\Pr\{PAPR > PAPR_0\}$ ). In Figure 5, the CCDF of PAPR of IFDMA, LFDMA and OFDMA are presented.

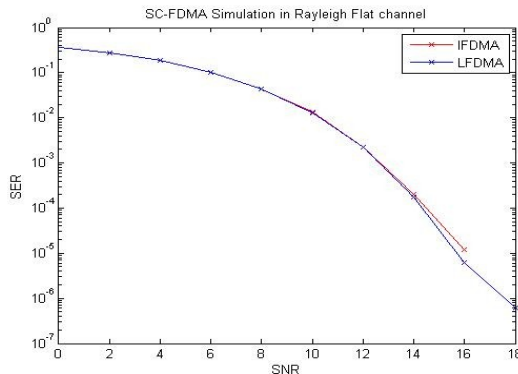


Figure 4. Comparison of SER IFDMA and LFDMA in flat fading Rayleigh channel.

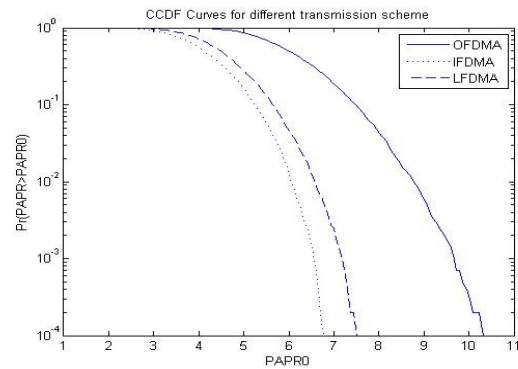


Figure 5: Comparison of CCDF of PAPR for IFDMA, LFDMA, and OFDMA with total number of subcarriers  $N = 512$ , and QPSK modulation.

We can see that both cases of SCFDMA have indeed lower PAPR than that of OFDMA. Also, it can be observed analyzing last figure that IFDMA has the lowest PAPR.

## 4. Peak-to-Average Power Ratio

In general, the PAPR of OFDM signals is defined as the ratio between the maximum instantaneous power and its average power:

$$PAPR[x(t)] = \frac{\max_{0 \leq t \leq NT} [|x(t)|^2]}{P_{av}} \quad (1)$$

The distribution of PAPR can be expressed in terms of CCDF. When  $N$  is large, the distribution of the output time vector converges to Gaussian due to Central Limit Theorem. Hence, as already said the probability that the PAPR is above a threshold  $\lambda$  can be written as:

$$\Pr\{PAPR > \lambda\} = 1 - (1 - e^{-\lambda})^N \quad (2)$$

## 4.1. Proposed PAPR reduction techniques

### 4.1.1. Pre-coding Techniques in OFDM systems for PAPR reduction

#### a. The Discrete Cosine Transform

Mathematically, the unitary Discrete Cosine Transform (DCT) of an input sequence  $x$  is:

$$y(k) = w(k) \sum_{n=1}^N x(n) \cos \frac{\pi(2n-1)(k-1)}{2N}, \quad k = 1, \dots, N \quad (3)$$

where the analysis window  $w$  can be expressed as:

$$w(k) = \begin{cases} 1/\sqrt{N} & , \quad k = 1 \\ \sqrt{2/N} & , \quad 2 \leq k \leq N \end{cases} \quad (4)$$

#### b. Zadoff-Chu sequences

Zadoff-Chu codes are the special case of the generalized Chip-Like polyphase sequences having optimum correlation properties [57]. Indeed, Zadoff-Chu sequences of length  $L$  offer an ideal periodic autocorrelation and a constant magnitude ( $\sqrt{L}$ ) periodic cross-correlation. They are defined by:

$$Z(k) = \begin{cases} e^{\frac{j2\pi r}{L}(\frac{k^2}{2} + qk)} & \text{for } L \text{ even} \\ e^{\frac{j2\pi r}{L}(\frac{k(k+1)}{2} + qk)} & \text{for } L \text{ odd} \end{cases} \quad (5)$$

where  $k=0, 1 \dots L-1$ ,  $q$  is any integer,  $r$  is the code index, prime with  $L$ . Consequently, if  $L$  is a prime number, the set of Zadoff-Chu codes is composed of  $L-1$  sequences.

#### c. Walsh-Hadamard Transform

Like the FFT, the Walsh–Hadamard transform has a fast version, the Fast Walsh–Hadamard Transform (FWHT). The FWHT is able to represent signals with sharp discontinuities more accurately using fewer coefficients than the FFT. Both the FWHT and the inverse FWHT (IFWHT) are symmetric and thus, use identical calculation processes. The FWHT and IFWHT for a signal  $x(t)$  of length  $N$  are defined as:

$$y_n = \frac{1}{N} \sum_{i=0}^{N-1} x_i \text{WAL}(n, i) \quad (6)$$

$$x_i = \frac{1}{N} \sum_{n=0}^{N-1} y_n \text{WAL}(n, i) \quad (7)$$

where  $i = 0, 1, \dots, N-1$  and  $WAL(n, i)$  are Walsh functions.

Finally, it must be mentioned the fact that the single carrier Frequency Division Multiplexing used in LTE in uplink is implemented by DFT pre-coding.

- **Simulation results**

The block implementation is shown in Figure 6, where the pre-coding matrix corresponds to different pre-coding techniques used in our simulations.

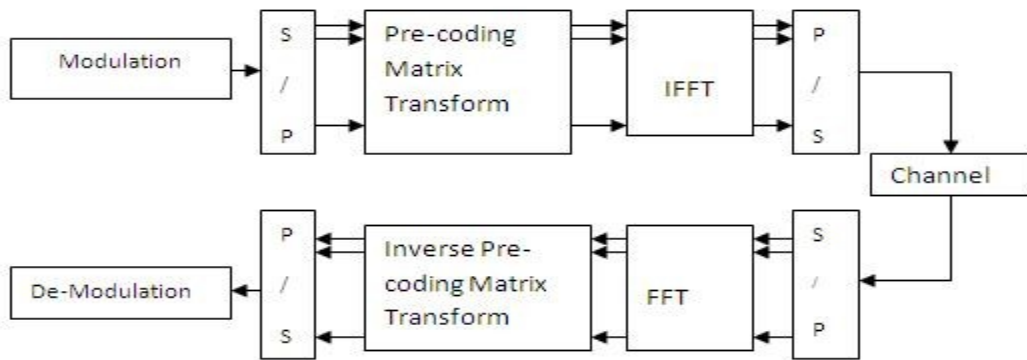


Figure 6: Block scheme of pre-coding technique in OFDM system.

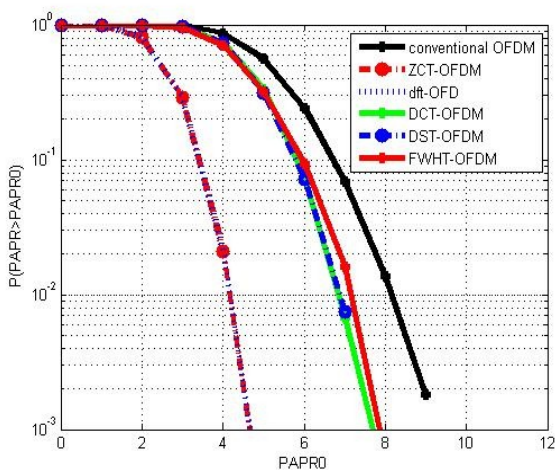


Figure 7: CCDF for different pre-coding techniques with 16 QAM.

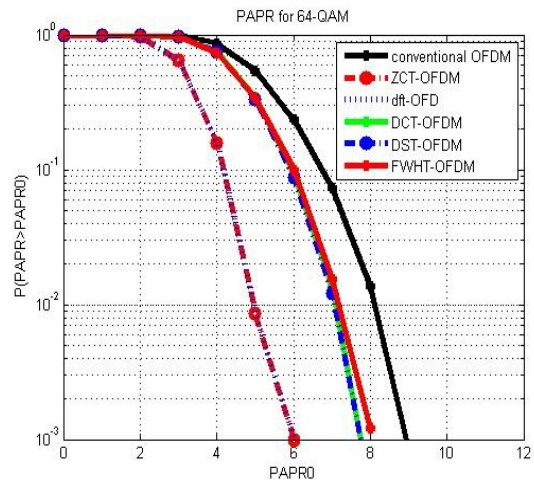


Figure 8: CCDF for different pre-coding techniques with 64 QAM.

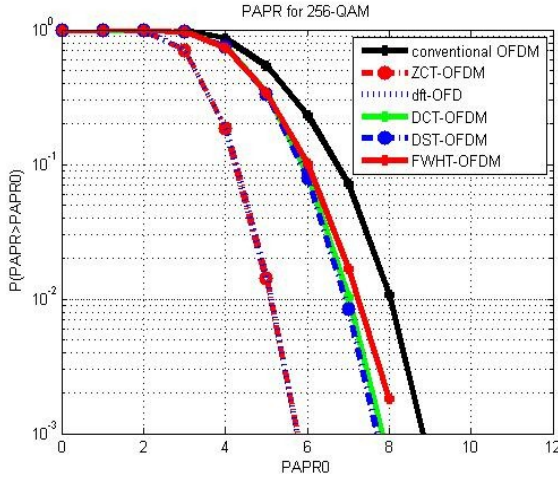


Figure 9: CCDF for different pre-coding technique with 256QAM.

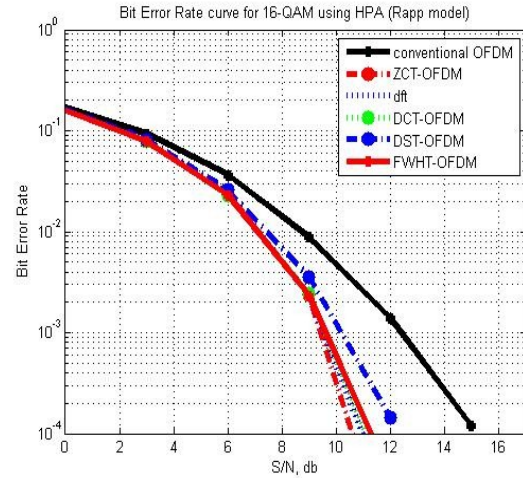


Figure 10: BER performances for OFDM with and without pre-coding techniques.

The encoding was realized in the transmitter before the computation of IFFT and the corresponding decoding was realized in the receiver after the computation of FFT. Figures 7, 8, and 9 represent the PAPR distributions obtained for different pre-coding techniques: DCT, Discrete Sine Transform (DST), Zadoff-Chu sequences (ZCT), FWHT and the Discrete Fourier Transform (DFT), with 16, 64, and 256 QAM. We can observe in Figure 8 that at CCDF= $10^{-2}$ , the PAPR is reduced by approximately 5.2 dB for DFT and Zadoff-Chu, by 1.8 dB for DCT and 1 dB for FWHT pre-coding based OFDM systems.

In Figure 10 are represented the BER performances of different pre-coding based OFDM systems using the HPA (Rapp model). We can observe that the pre-coding based OFDM systems compensate the non-linearities introduced by HPA and have better performance than simple OFDM system.

#### 4.1.2. Combined Partial Transmit Sequence and Companding for PAPR Reduction in OFDM Systems

The proposed technique is shown in Figure 11.

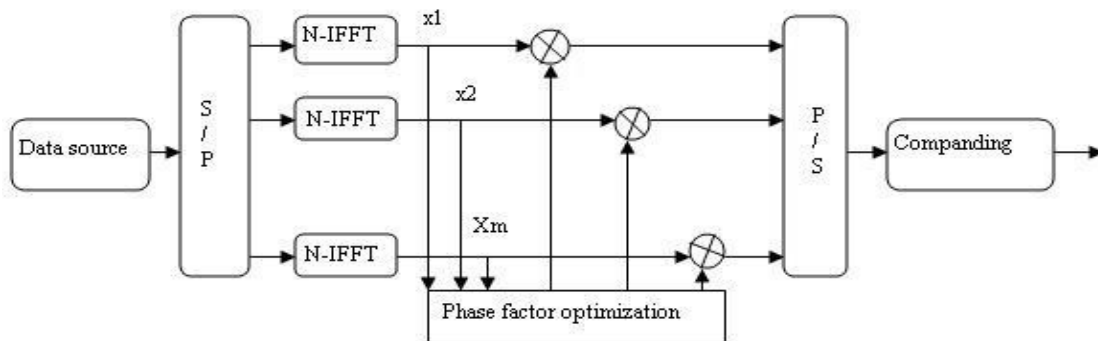


Figure 11: Block diagram of the proposed PAPR reduction method based on combining PTS and Companding techniques.

The main idea of the proposed scheme is to use a combination of two PAPR reduction methods. First, the PTS approach is used and second the signal with the lowest PAPR is submitted to the companding technique. The results presented in the following were obtained by considering an Additive White Gaussian Noise (AWGN channel, 512 subcarriers and a QPSK modulation).

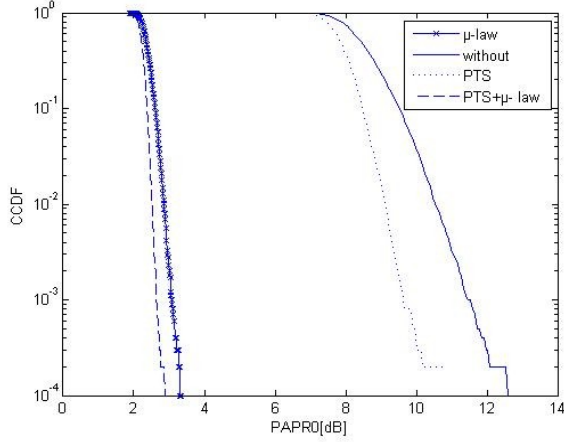


Figure 12: CCDF performance for different PAPR reduction techniques. For the proposed method a value of  $\mu = 255$  was used.

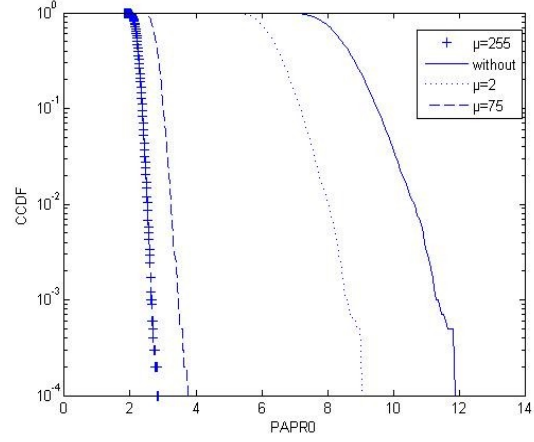


Figure 13 CCDF performance of the proposed method for different values of  $\mu$ .

The simulation results obtained prove the good performance of the approach proposed, better than the performance that can be obtained using only one of the two composing methods applied separately.

#### 4.1.3. PAPR reduction Using Soft Reduction Comanding for SC-FDMA

We proposed a new PAPR reduction scheme based on combining the Soft Reduction transform and Comanding system. It can be implemented in SC-FDMA system at the Cyclic Prefix output. Figure 14 presents the principle of the A-law/ $\mu$ -Law soft reduction technique (ASR/ $\mu$ SR).

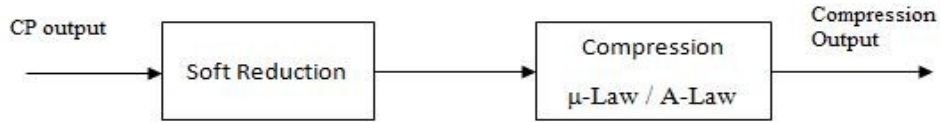


Figure 14: Soft reduction compressor.

First the soft reduction transform is applied to the CP output  $x$ , the resulting signal can be written as:

$$x_{SR} = \frac{x}{(1+x^2)^{1/2}} \quad (8)$$

Then we apply the A-Law compressor on the soft reduction output  $x_{SR}$  in order to obtain the following signal:

$$Y_{ASR} = \begin{cases} \frac{1+\log(A|x_{SR}|)}{1+\log A} \operatorname{sgn}(x_{SR}); & \frac{1}{A} \leq |x_{SR}| \leq 1 \\ \frac{A|x_{SR}|}{1+\log A} \operatorname{sgn}(x_{SR}); & 0 \leq |x_{SR}| \leq \frac{1}{A} \end{cases} \quad (9)$$

where  $A$  is the compression parameter. The custom value of  $A$  used in Europe is of 87.6.

We can also use the  $\mu$ -Law compressor which has the same basic features and implementation advantages as the A-Law compressor. In order to verify the performance of the proposed companding scheme, we simulated the SC-FDMA system with parameters presented in the following table.

Table 1: Simulation parameters.

Total number of subcarriers	512
Subcarrier mapping scheme	LFDMA
Channel	AWGN
Channel estimation	MMSE
Modulation	QPSK and 16QAM

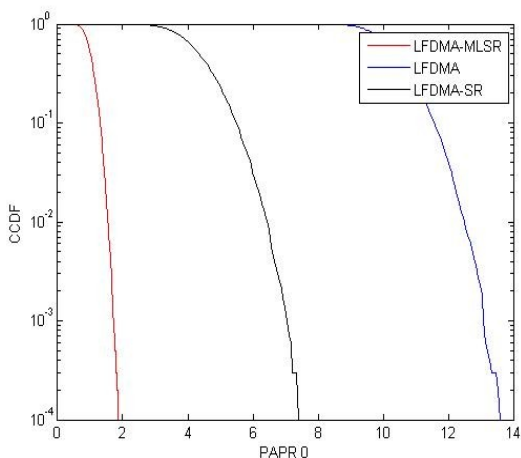


Figure 15: CCDF performance of LFDMA with  $\mu$ -Law compressor and Soft reduction.

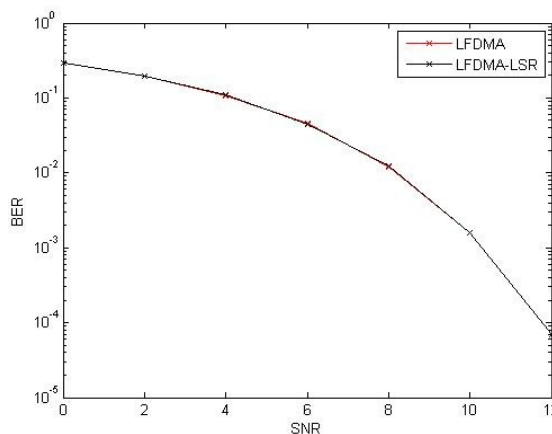


Figure 16: BER performance of the LFDMA with the proposed scheme in comparison with the original LFDMA system

Figure 15 shows the Complementary Cumulative Distribution Function of the PAPR with the proposed reduction scheme. With this scheme, the PAPR was reduced by 12 dB at  $CCDF=10^{-4}$ . We also analyzed also the BER of LFDMA with our companding function and we presented the BER performance in Figure 16 where BER performance is compared to simple LFDMA. We can easily observe that this companding function produce no BER degradation. As a conclusion, by a simple PAPR reduction technique, we obtained good PAPR result without deteriorating the BER curves and this is the principle goal.

## 5. Channel Estimation

### 5.1. Blind Channel Estimation Technique Based on Denoising for LTE Downlink and Uplink system

The goal of this technique is to perform blind estimation based on denoising for LTE in UL and DL. The idea of this technique comes from a paper published by Professor David Donoho from Stanford University in 1992, which introduced the term denoising in connection with the adaptive non-linear filtering applied in the wavelets domain, [82]. This paper produced a high interest in the world of science and represents a source of inspiration for a huge number of papers, which were already published and

continue to appear. Despite its advantages, this method was not systematically exploited in communications yet.

Let us suppose that the signal  $s[k]$  is additively perturbed by the white Gaussian noise  $n[k]$ . This is the well known scenario of the AWGN channel. The received signal has the expression:  $x[k]=s[k]+n[k]$ . The denoising method is based on the following three steps method:

1) Computation of the Discrete Wavelet Transform (DWT) of the signal  $x[k]$  obtaining the wavelet coefficients sequence,  $y[k] = s[k] + n[k]$ , where the noise  $n[k]$  is white and Gaussian (WGN) [83]. The approximation  $y_{ia}$  and details  $y_{id}$  sequences are separated.

2) A non-linear filtering is applied to the sequence of detail coefficients obtained:

$$y_{0d}[k] = \begin{cases} \text{sgn}\{y_{id}[k]\}(|y_M[k]| - t), & |y_M[k]| > t \\ 0, & \text{if not} \end{cases} \quad (10)$$

where  $t$  is a threshold.

3) The approximation coefficients sequence  $y_{ia}$  is concatenated with the new detail coefficients sequence  $y_{0d}$  obtaining the new sequence of wavelet coefficients  $y_0$  and is computed its inverse DWT (IDWT). The estimation of the signal  $s[k]$ , denoted by  $s_0[k]$ , is obtained.

The non linear filter applied at the second step is named soft-thresholding. The idea of the proposed technique is the inclusion of a denoising system in the chain of wireless receiver based on OFDMA and SC-FDMA, to improve their Bit Error Rate (BER) . The architecture of the proposed blind estimator is presented in Figure 17. The blind estimation is performed after IDFT computation in OFDMA and DFT computation in SC-FDMA at the receiver of each scheme. The proposed denoising system implements the simplified variant of the Donoho's denoising method, without filtering, which consist in meting all the DWT detail coefficients to zero.



Figure 17: The architecture of the proposed blind estimation system.

The blind estimator is implemented with the aid of an interpolator (Upsampling system in Figure. 17) with an interpolation factor of 8. So, our blind estimation system is composed by the interpolator, followed by the denoising system and by down sampling system having the down sampling factor of 8. This last system selects each of the fourth samples from a group of 8 consecutive samples of its input signal.

- **Simulation results**

We have considered SISO system. The OFDMA and SC-FDMA transmission chain already described including or not the blind Estimation (BE)was simulated, we used QPSK modulation and flat fading Rayleigh channel model. For subcarrier mapping in SC-FDMA, we simulated the IFDMA scheme. The denoising was performed using DWT computed with the Haar mother wavelets for six iterations, and We performed the simulations in Matlab, in order to evaluate the performance of the proposed blind estimation technique.

Figure 18 shows a comparison of BER performance of SC-FDMA communication system equipped or not equipped with blind estimation technique. At SNR=3 dB, the BER is approximately 0.0002 when the blind estimation technique is used and about 0.005 without the proposed technique. At BER equal to 0.0001, the gain of SC-FDMA equipped with the blind estimation based on denoising is about 6 dB. These results prove also the good performance of the proposed technique.

Figure 19 shows a comparison of BER performance of an OFDMA system equipped or not with the proposed blind estimation technique. Comparing the experimental results, it can be observed that the blind estimation improves substantially the performance of both types of communication systems, so the contribution of this technique is very important. The proposed blind estimation method is simpler than the non blind estimation methods, because it does not require the channel estimation. It could be used for channel estimation as well for both OFDMA and SC-FDMA which are used in LTE technology. The DWT computation algorithm implemented with the Haar mother wavelets is faster than the FFT algorithm. The soft thresholding filter is also very fast. So, the blind estimation method proposed in this paper is faster than the non blind estimation methods which are based on iterative algorithms and permits the tracking of faster time varying channels. The simulation results presented highlight the very good quality of the proposed estimation method outperforming the results obtained using other equalization methods as for example the zero forcing method. Such results can be obtained on AWGN channels only with the aid of coding techniques which are redundant and require important computing resources.

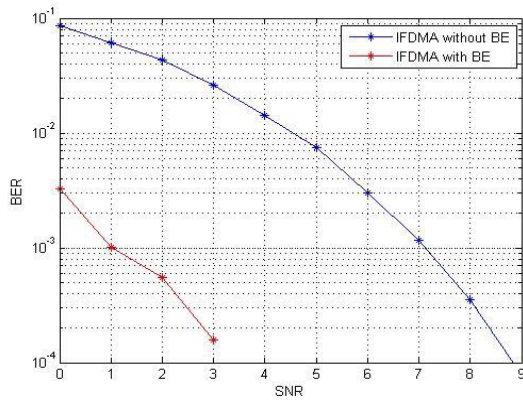


Figure 18: A comparison of the performance BER (SNR) obtained with and without blind estimation in SC-FDMA (IFDMA) system

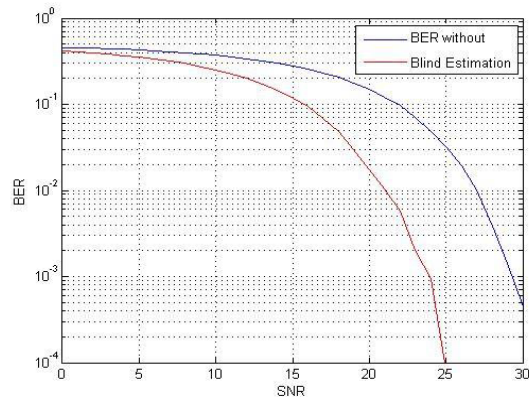


Figure 19: A comparison of the performance BER (SNR) obtained with and without blind estimation in OFDMA system.

## 6. Conclusions

In this work, we analyzed and compared the multiple access schemes in 3GPP LTE in downlink and uplink, using simulation in Matlab; we also investigated some precoding techniques used in OFDM systems for PAPR reduction and we proposed two PAPR reduction techniques; we have designed a new blind estimation technique based on denoising for the uplink and downlink in LTE. We have also implemented and simulated this technique in both OFDMA and SC-FDMA scenarios by considering SISO system. We have shown, by simulation, that the blind estimation improves substantially the performance of both types of communication systems.